

NUCLEAR CONCENTRATION OF MOLECULAR GAS IN THE LATE-TYPE SPIRAL GALAXY NGC 6946: 300 PARSEC SCALE GASEOUS DISK

S. ISHIZUKI,¹ R. KAWABE,² M. ISHIGURO,² S. K. OKUMURA,^{1,2} K.-I. MORITA,² Y. CHIKADA,²
 T. KASUGA,² AND M. DOI¹

Received 1989 July 28; accepted 1989 December 5

ABSTRACT

The CO ($J = 1-0$) emission in the central 65" (1.7 kpc) region of the nearby late-type spiral galaxy NGC 6946 has been mapped using the Nobeyama Millimeter Array (NMA). The synthesized beam is $7''.6 \times 4''.2$ (HPBW) which corresponds to 200 pc \times 110 pc at the distance of 5.5 Mpc. We have found a massive nuclear concentration of molecular gas with a scale of 300 pc and a molecular bar structure elongated more than 1.5 kpc. The velocity structure suggests that the molecular gas in the nuclear concentration has a circular rotation and the gas in the molecular bar structure has an infall motion. The total H₂ mass in the central 65" region is $(4 \pm 2) \times 10^8 M_{\odot}$, 75% [$(3 \pm 1.5) \times 10^8 M_{\odot}$] of which was found in the 300 pc scale nuclear concentration. The averaged molecular gas density is estimated to be as high as $(2 \pm 1) \times 10^3 \text{ H}_2 \text{ cm}^{-3}$ in the nuclear concentration. The region of the central concentration coincides with a bright H II region and a radio continuum source. It is suggested that the nuclear concentration is a massive nuclear disk of molecular gas which has been formed by efficient gas inflow in an oval potential field, and the high H₂ density supports active star formation in the nuclear region.

Subject headings: galaxies: individual (NGC 6946) — galaxies: internal motions —
 galaxies: interstellar matter — galaxies: nuclei — galaxies: structure

I. INTRODUCTION

Bar structures of molecular gas are found with high spatial resolution observations at the central 2–3 kpc regions of the late-type spiral galaxies IC 342 (Lo *et al.* 1984), NGC 6946 (Ball *et al.* 1985), NGC 253 (Canzian, Mundy, and Scoville 1988), and Maffei 2 (Ishiguro *et al.* 1989). The bar structures have been interpreted as a part of shock waves at the leading edges in stellar gravitational potential with oval distortion (e.g., Sørensen, Matsuda, and Fujimoto 1976; Roberts, Huntley, and van Albada 1979). Molecular gas loses its angular momentum mainly at the shock regions and falls into the nuclear region. These bar structures are suggested to fuel nuclear region to cause starburst activities. It is also suggested that in starburst galaxies such as M82 and NGC 253 there exist stellar bars which would trigger starbursts (Lo *et al.* 1987; Scoville *et al.* 1985).

NGC 6946 is a late-type spiral galaxy classified as Sc(s)II by Sandage and Tammann (1981) and as SABcd by de Vaucouleurs, de Vaucouleurs, and Corwin (1976). The distance to NGC 6946 is 5.5 Mpc (Tully 1988), and all values quoted in this paper from previous works have been scaled to this distance. Parameters for NGC 6946 are summarized in Table 1.

CO in NGC 6946 has been studied by many authors. Young and Scoville (1982) observed using the FCRAO 14 m antenna and found the exponential CO disk component between radii of 2 kpc and 14 kpc. Ball *et al.* (1985) mapped the galaxy using the Owens Valley Millimeter-Wave Interferometer with the synthesized beam of $7''.6 \times 5''.4$ (HPBW) and found a molecular bar with a extent of 1500 pc \times 300 pc. However, their velocity coverage was 83 km s^{-1} which was only one-third of the full velocity width of the CO emission. Wellichew, Casoli, and

Combes (1988) made observations using the IRAM 30 m telescope with a 23" beam and found unresolved nuclear component of H₂ mass of $1.7 \times 10^8 M_{\odot}$ within their beam size 600 pc in diameter. They also suggested the bar structure from the elongated shape of a rectified CO intensity map. Using the Nobeyama 45 m telescope, Sofue *et al.* (1988) found an unresolved CO molecular gas core in the center and the distortion of the velocity field suggesting an oval potential field.

We have made aperture synthesis observations of CO ($J = 1-0$) emission from the central region [1.7 kpc (65") in diameter] of NGC 6946 using the Nobeyama Millimeter Array. The beam width is $7''.6 \times 4''.2$ at HPBW, and the velocity coverage is 830 km s^{-1} which sufficiently covers the velocity width of the CO emission ($\sim 220 \text{ km s}^{-1}$). We have found a massive nuclear concentration of molecular gas which is interpreted as a nuclear disk inside the molecular bar. In this paper, we will present the results and discuss the nature of the nuclear molecular disk and the molecular bar, their formation mechanisms, and star formation in the disk.

II. OBSERVATIONS

The central region (1.7 kpc in diameter) of NGC 6946 was observed in the $J = 1-0$ line of CO (115.271 GHz) using the Nobeyama Millimeter Array (NMA) (Ishiguro *et al.* 1984, 1990) on 1988 May 5 and 9. The array consists of five 10 m antennas which are equipped with SIS receivers (Kawabe *et al.* 1990). The system noise temperatures (SSB) were 600–700 K at the zenith. An FFT spectro-correlator with 1024 channels called an FX (Chikada *et al.* 1987) was used. The bandwidth was 320 MHz, which corresponds to a velocity coverage of 832 km s^{-1} at 115 GHz. The velocity resolution was 0.81 km s^{-1} .

The observations were made using a single array configuration with 10 baselines. The projected baseline lengths ranged from 19.4 m (7.5 λ) to 68.5 m (26.3 λ). Structures larger than 28" were not sampled. The synthesized beam was $7''.6 \times 4''.2$

¹ Department of Astronomy, University of Tokyo.

² Nobeyama Radio Observatory (NRO), National Astronomical Observatory. Nobeyama Radio Observatory is a branch of the National Astronomical Observatory, the Ministry of Education, Science and Culture of Japan.

TABLE 1
PARAMETERS FOR NGC 6946

Parameter	Value	Reference
R.A. (1950)	20 ^h 33 ^m 49 ^s .2	1
Decl. (1950)	59°58'49".5	1
Distance	5.5 Mpc	2
Systemic velocity $V_{\text{LSR}}^{\text{sys}}$	60 km s ⁻¹	...
Morphological type	Sc(s)II	3
	SABcd	4
P.A. of the major axis	62°	5
Inclination	30°	5

REFERENCES.—(1) Turner and Ho 1983; (2) for the distance to NGC 6946, various values are used in literature; 10.1 Mpc (e.g., Rogstad and Shostak 1972), 7 Mpc (e.g., Klein *et al.* 1982), 5.1 Mpc (e.g., Weliachew, Casoli, and Combes 1988), and 5.5 Mpc (Tully 1988). We adopted the most recent value: 5.5 Mpc; (3) Sandage and Tammann 1981; (4) de Vaucouleurs, de Vaucouleurs, and Corwin 1926; (5) Rogstad and Shostak 1972.

(HPBW) with a position angle (P.A.) of 147° which corresponds to about 200 pc × 110 pc at the distance of 5.5 Mpc.

We observed BL Lac for 10–15 minutes every 30 minutes in order to calibrate instrumental gain and phase. The total on-time of NGC 6946 was 291 minutes. The flux density of BL Lac at 115 GHz was estimated to be 4.5 ± 0.5 Jy from observations of Uranus, assuming that the brightness temperature of Uranus at 115 GHz estimated from the measurements by Ulich (1981) at $\lambda = 3.3$ mm and Gear *et al.* (1984) at $\lambda = 0.4$ –2.0 mm is 120 K. The bandpass across the 1024 frequency channels was determined from the 30–60 minute observations of 3C 84.

CO maps were made and CLEANed in the conventional manner using the NRAO AIPS package. The rms noise level of the maps with a velocity width of 19.5 km s⁻¹ was about 0.27 Jy beam⁻¹ which corresponds to 0.78 K in brightness temperature. The maps shown in this paper were not corrected for primary beam attenuation. The observational parameters are summarized in Table 2.

III. RESULTS

Figure 1a shows a map of integrated CO intensity, $\int T_B(v)dv$, over a velocity width, 219.4 km s⁻¹, which covers almost all of

CO emission from NGC 6946 (Young and Scoville 1982). The rms noise level of the map is $\sigma = 42$ K km s⁻¹ in integrated CO intensity. A cross in Figure 1a indicates the galactic nucleus determined from the peak of radio continuum emission observed by Turner and Ho (1983). Two features can be seen in the CO map: one is a nuclear concentration, the other is a diffuse feature with north-south extension of about 1'. The total extension of CO emission may be larger than 65" (1.7 kpc) because the field of view is limited by primary beam attenuation. The diffuse feature corresponds to a barlike structure seen in Figure 1b.

To see the north-south diffuse feature more clearly, we have summed four channel maps (Figs. 3e–3h) at a velocity range, $V_{\text{LSR}} = +21.4$ – $+99.5$ km s⁻¹. The result is shown in Figure 1b, in which the nuclear concentration and an offset barlike structure is remarkable. The size of the barlike structure in the plane of the galaxy is 800 pc in the northern part and 600 pc in the south. The offset newly found is toward the leading side if we assume trailing spiral arms in NGC 6946. The orientation of the barlike structure is roughly consistent with that obtained by Ball *et al.* (1985) and that in the rectified map by Weliachew, Casoli, and Combes (1988).

Figure 1c is a map of mean velocities, $\sum v \cdot T_B(v) / \sum T_B(v)$, which is made from channel maps shown in Figure 3. In the calculation, brightness temperatures lower than 1.2 K (1.5 σ noise level) in the channel maps are excluded in order for the map not to be contaminated by noise components. Inside the radius 5" of the nuclear concentration, the P.A. of the isovelocity contour at the systemic velocity $V_{\text{LSR}} = 60$ km s⁻¹ is $141^\circ \pm 2^\circ$, which is very close to the position angle of the minor axis of the galaxy determined from the kinematics in the disk, P.A. = $152^\circ \pm 5^\circ$ (Rogstad and Shostak 1972). The isovelocity contours in the nuclear region indicate that the central concentration is a circularly rotating disk. Hereafter, we call it *the nuclear molecular disk*. If the skewness between them, $11^\circ \pm 5^\circ$, is real, it means the existence of a noncircular motion (expanding motion if trailing spiral arms are assumed) in addition to the circular rotation.

The isovelocity contours at the northern and southern barlike features are largely distorted from those expected from a circular rotation. The northern and southern barlike structures have redshifted and blueshifted velocities, respectively, with respect to those expected in case of a circular rotation. This indicates that a noncircular motion of the gas exists in the

TABLE 2
OBSERVATIONAL PARAMETERS

Parameter	Value
Observing period	1988 May 5 and 9
Frequency	CO ($J = 1-0$) 115.271 GHz ($\lambda 2.6$ mm)
Integration time (on source)	156 minutes on May 5 135.5 minutes on May 9
Bandwidth	320 MHz (832 km s ⁻¹)
Maximum baseline length	68.5 m (26.3 k λ ; projected) 19.4 m (7.5 k λ ; projected)
Synthesized beam	7".6 × 4".2 (FWHM) (200 pc × 110 pc at 5.5 Mpc)
Position angle	147°
Field of view	65" (1.7 kpc) (HPBW)
Phase center	
α	20 ^h 33 ^m 49 ^s .5
δ	59°58'45".0
Reference calibrator	BL Lac
Bandpass calibrator	3C 84
Flux calibrator	Uranus ($T_b = 120$ K)

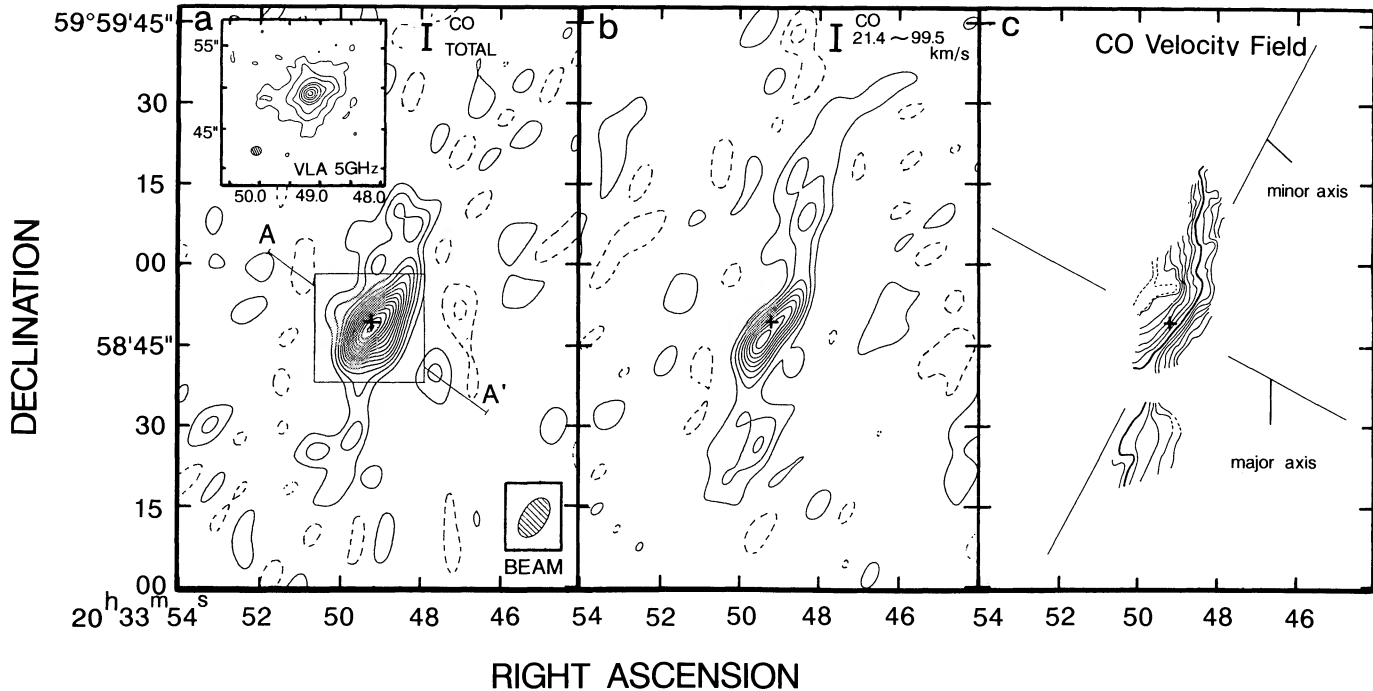


FIG. 1.—(a) A map of total CO intensity integrated over 219.5 km s^{-1} , from $V_{\text{LSR}} = -49.2 \text{ km s}^{-1}$ to $+170.2 \text{ km s}^{-1}$. A contour interval is 63 K km s^{-1} (1.5σ noise level of the map). A contour with a zero level is not shown in the maps. A map in the upper left panel is a map of 6 cm radio continuum emission from the central region (shown by a frame) obtained by Turner and Ho (1983). A cross indicates the peak of the radio continuum map. (b) A map of CO integrated intensity in the velocity range, $V_{\text{LSR}} = +21.4 \sim +99.5 \text{ km s}^{-1}$. A contour interval is 46 K km s^{-1} (1.5σ). (c) A contour map of a mean velocity, $\sum v T_B(v) / \sum T_B(v)$. Dashed lines indicate contours at $V_{\text{LSR}} = -20$ and -10 km s^{-1} , and solid lines at $V_{\text{LSR}} = 0, 10, \dots, 120 \text{ km s}^{-1}$ from east to west. A thick solid line indicates a contour at the systemic velocity, $V_{\text{LSR}}^{\text{sys}} = 60 \text{ km s}^{-1}$.

barlike structure. If the gas is in the plane of the galaxy and the spiral arms are trailing arms, the northwest side of the disk inclines to the nearer side and the noncircular motion is an infall motion (or a pair of inward motions in oval rotation). The “infall velocity” is about $60\text{--}80 \text{ km s}^{-1}$ in the plane. At the northwest end of the nuclear concentration, the isovelocity contours are distorted and connect to those in the barlike structure. This region is likely the interface of the barlike structure and the nuclear disk. Here, we define the size of the nuclear disk as an extent of the region of a circular rotation, which is 300 pc in diameter if it is projected to the disk plane.

Figure 2 shows a position-velocity diagram along a line with P.A. = 50° (A–A' in Fig. 1a), which is almost perpendicular to the isovelocity contour for the systemic velocity. This map indicates the presence of a rigid-body rotation within $3''$ ($\sim 75 \text{ pc}$) from the nucleus and a flat rotation outside the region. The velocity gradient projected to the plane of the galaxy is $1.9 \text{ km s}^{-1} \text{ pc}^{-1}$ if a circular rotation is assumed.

Figure 3 shows channel maps with a velocity width of $\Delta V = 19.5 \text{ km s}^{-1}$. The rms noise level of each channel map, σ , is about 15 K km s^{-1} . Components corresponding to the nuclear disk are seen throughout the maps (Figs. 3b–3k) with velocities between $V_{\text{LSR}} = -17.6 \text{ km s}^{-1}$ and 138.5 km s^{-1} . The north-south diffuse barlike feature is seen in the maps (Figs. 3d–3i) with velocities between $V_{\text{LSR}} = +1.9 \text{ km s}^{-1}$ and $V_{\text{LSR}} = +119.0 \text{ km s}^{-1}$. Strong peaks in the nuclear disk are shifted to the southeast (see Figs. 3d–3g) and northwest (see Fig. 3h) of the nucleus at velocities smaller and larger than $V_{\text{LSR}} = 80.0 \text{ km s}^{-1}$, respectively. Each shift is toward each inner end of the barlike structure. The elongated emission is located at $9''$ (240 pc) northeast of the nucleus (Fig. 3b) and

$15''\text{--}18''$ ($400\text{--}480 \text{ pc}$) southwest (Figs. 3j and 3k). They correspond to the region of a flat rotation in the position-velocity map (Fig. 2) and are probably the outer parts of the nuclear disk.

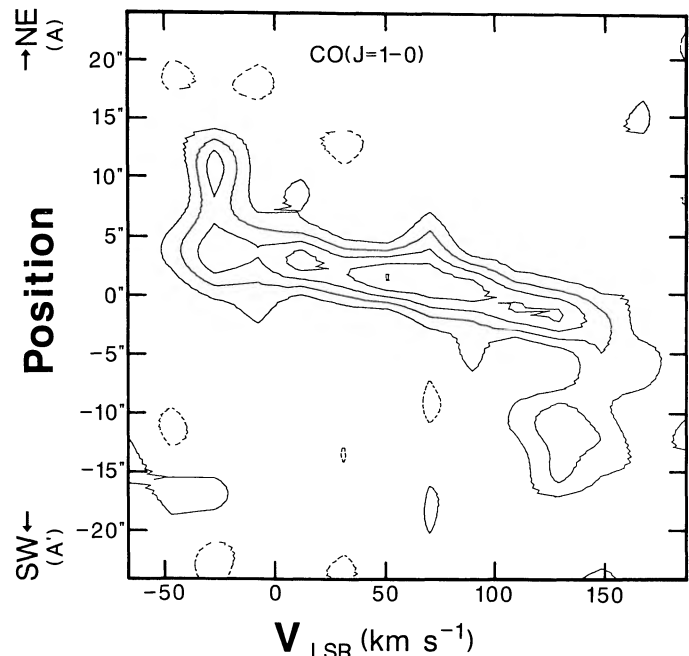


FIG. 2.—A position-velocity map along a cut $50''$ long (A–A') shown in Fig. 1a. A contour interval is 1.2 K .

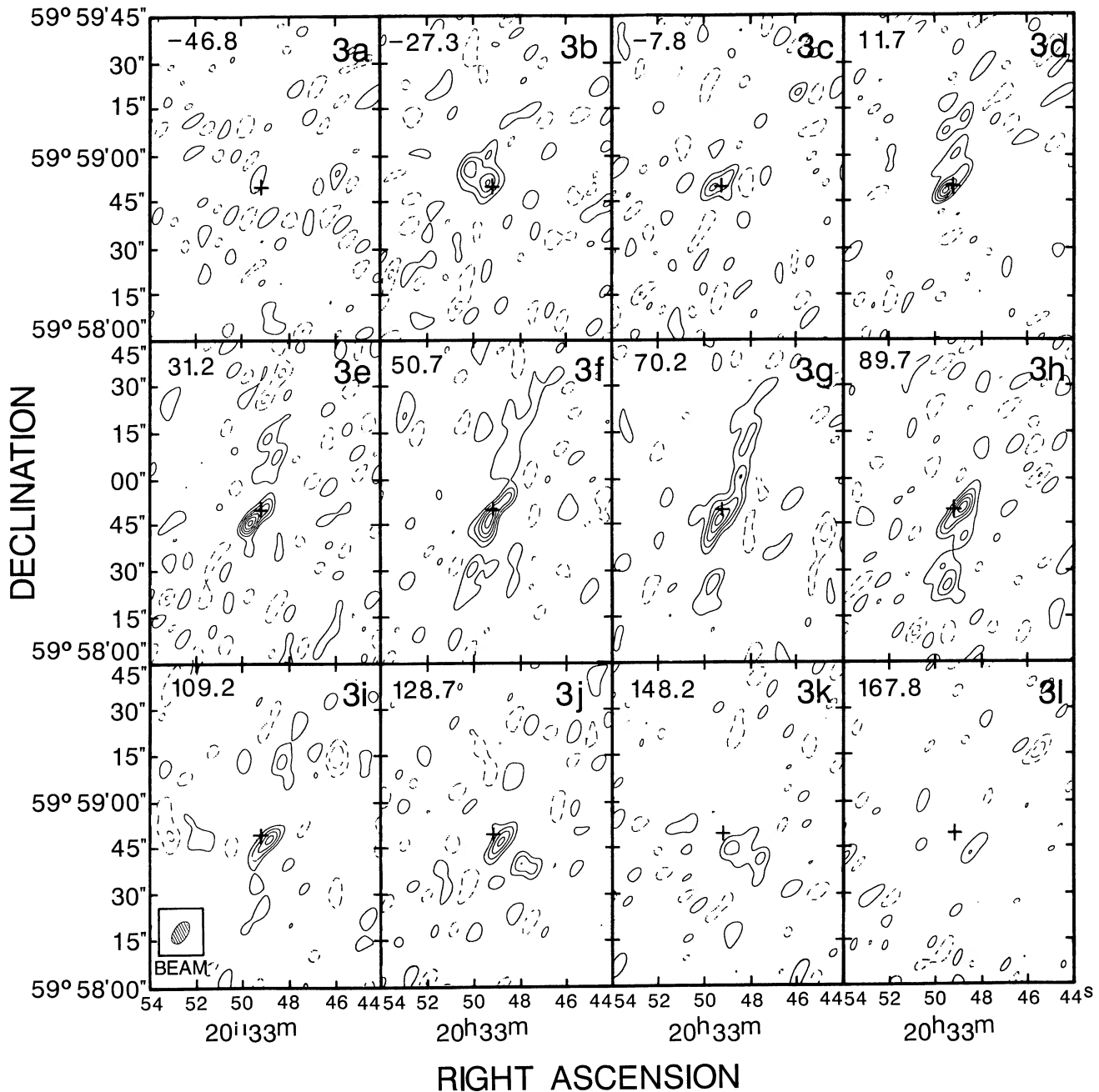


FIG. 3.—CO channel maps with a velocity width of 19.5 km s^{-1} from $V_{\text{LSR}} = -46.8$ to $+167.8 \text{ km s}^{-1}$. A contour interval is 23 K km s^{-1} . Each center velocity (in km s^{-1}) is indicated in each panel. A cross has the same meaning as in Fig. 1a.

IV. DISCUSSION

a) Total Mass of Molecular Gas

We estimate the total mass of molecular gas in the central $65''$ (1.7 kpc) region from observed CO intensities. The total flux density, $\langle F \rangle$, averaged over a velocity width of $\Delta V = 219.4 \text{ km s}^{-1}$ is 6.3 Jy . The total CO flux $1380 \text{ Jy km s}^{-1}$ is 72% and 71% of the total CO fluxes in the central $65''$ region which we estimated using the CO maps by single-dish observations by Weliachew, Casoli, and Combes (1988) and Sofue *et al.* (1988), respectively. If we consider the primary beam attenu-

ation and the lack of short spatial frequencies in our interferometric observation, they are in good agreement.

The column density of hydrogen molecule can be estimated using the conversion equation between CO intensity and the H_2 column density. The equation derived by Young and Scoville (1982) for dark nebulae and giant molecular clouds in our Galaxy with the FCRAO 14 m telescope is $\sigma(\text{H}_2) = (6 \pm 3) \times (I_{\text{CO}}/\text{K km s}^{-1}) M_{\odot} \text{ pc}^{-2}$, where $I_{\text{CO}} = \int T_{\text{A}}^* dV$ (T_{A}^* is in NRAO scale; $T_{\text{A}}^* = 0.65 T_{\text{B}}$). The H_2 mass is obtained as $M(\text{H}_2) = (10,000 \pm 5000) \times \langle F \rangle \Delta V D_{\text{Mpc}}^2 (\lambda/2.6 \text{ mm})^2 M_{\odot}$, where D_{Mpc} is the distance to the galaxy in units of Mpc. The

total H_2 mass is $(4 \pm 2) \times 10^8 M_\odot$. For the nuclear molecular disk, $\langle F \rangle = 4.8$ Jy, and $M(H_2)$ is estimated to be $(3 \pm 1.5) \times 10^8 M_\odot$, which is about 10% of mass of molecular gas within a radius of 8 kpc in NGC 6946 observed by Young and Scoville (1982). This indicates the strong concentration of molecular gas in the nuclear 300 pc region.

These H_2 masses are overestimated if the molecular clouds are optically thin in the CO ($J = 1-0$) line (Knapp *et al.* 1980) or its excitation temperature is as high as in hot core regions like Orion KL (Young and Scoville 1982). In the nuclear region of NGC 6946, it was suggested that molecular clouds are optically thick because the ratio of the brightness temperatures of the CO ($J = 1-0$) and CO ($J = 2-1$) lines is close to unity (Lo *et al.* 1980). The dust temperature obtained by Rickard and Harvey (1984) is 36 K, and the excitation temperature of the CO ($J = 1-0$) line can be considered as small as this value. Therefore, the effects of the opacity and the excitation temperature on overestimation is probably small.

b) The Nature of the Nuclear Molecular Disk

From the H_2 mass of the nuclear disk, $M_{\text{tot}} = (3 \pm 1.5) \times 10^8 M_\odot$, an averaged H_2 number density is estimated to be about $(2 \pm 1) \times 10^3 H_2 \text{ cm}^{-3}$ in the disk with a radius of 150 pc if we assume that the thickness of the nuclear disk is the same as our Galaxy, 45 pc (Bally *et al.* 1988), and the density is uniform in the disk. The dynamical mass, M_{dyn} , can be estimated from the position-velocity diagram (Fig. 2). At a distance of 150 pc from the nucleus, the velocities relative to the systemic velocity are $\pm 90 \text{ km s}^{-1}$ which correspond to a rotation velocity of 180 km s^{-1} projected on the disk. Using an equation for spherically symmetric mass distribution, $M_{\text{dyn}} = 2.3 \times 10^2 (R/\text{pc}) (V/\text{km s}^{-1})^2 M_\odot$, the dynamical mass inside the radius $R = 150$ pc is derived as $1.1 \times 10^9 M_\odot$. Thus, the ratio of H_2 mass to the dynamical mass inside 150 pc is 0.28 ± 0.14 . This ratio is (9 ± 4) times higher than that estimated inside a radius of 11 kpc (Young and Scoville 1982). When one deconvolves the position-velocity diagram (Fig. 2) assuming the velocity gradient obtained in § III, one obtains an upper limit of rms internal velocity dispersion along the line of sight $\sigma_{v,\parallel}$, 34 km s^{-1} .

At the nuclear region, the peak brightness temperature of the CO ($J = 1-0$) line, T_B^{peak} , is about 6 K (see Fig. 2) and the CO line is optically thick (see § IVa). So, the filling factor in a synthesized beam is estimated to be $f = T_B^{\text{peak}}/[J(T_{\text{ex}}) - J(T_{\text{bg}})] \sim 6 \text{ K}/[J(36 \text{ K}) - J(3 \text{ K})] \sim 0.18$, where T_{ex} , a CO excitation temperature, is assumed to be equal to a dust temperature derived from infrared observations (with $50''$ aperture) by Rickard and Harvey (1984), T_{bg} is the temperature of the cosmic background radiation, and $J(T) = (hv/k)[\exp(hv/kT) - 1]$.

Using the derived beam-filling factor with the assumption that $T_{\text{ex}} = 36 \text{ K}$ and assuming that the nuclear molecular disk is composed of a number of identical molecular clouds with a spherical shape, the H_2 density in each cloud

$$\rho_{\text{cl}} = M_{\text{cl}}/[(4/3)\pi r^3]$$

can be estimated. Here we assume the mass of a cloud to be $M_{\text{cl}} = 5 \times 10^5 M_\odot$ (see e.g., Sanders, Scoville, and Solomon 1985). r is the radius of a cloud,

$$r = (\sigma_{\text{cl}}/\pi)^{1/2},$$

where σ_{cl} is the area of the cross section of a cloud. If we assume that the clouds are not overlapped along a line of sight,

σ_{cl} can be written as

$$\sigma_{\text{cl}} = fS \cos i/N_{\text{cl}},$$

where S is the surface area of the nuclear molecular disk ($S = \pi R^2$), i is the inclination of the galaxy, 30° , and $N_{\text{cl}} = M_{\text{tot}}/M_{\text{cl}}$ is the number of the molecular clouds contained in the nuclear molecular disk. The radius of a cloud is given as

$$r = 2.0 \times \left(\frac{f}{0.18}\right)^{1/2} \left(\frac{M_{\text{cl}}}{5 \times 10^5 M_\odot}\right)^{1/2} \left(\frac{M_{\text{tot}}}{3 \times 10^8 M_\odot}\right)^{-1/2} \text{ pc},$$

and the H_2 number density in a cloud is

$$n_{\text{cl}} = 1.7 \times 10^5 \left(\frac{M_{\text{cl}}}{5 \times 10^5 M_\odot}\right)^{-1/2} \left(\frac{f}{0.18}\right)^{-3/2} \times \left(\frac{M_{\text{tot}}}{3 \times 10^8 M_\odot}\right)^{3/2} H_2 \text{ cm}^{-3}.$$

These values imply that the molecular clouds at the nuclear disk are very compact and dense comparing with the giant molecular clouds in our Galactic disk. The density agrees with that obtained in the 30 pc region of the Galactic center ($\sim 10^5 H_2 \text{ cm}^{-3}$; Bally *et al.* 1988). Note that these conclusions are hold only under the assumptions adopted (a kinetic temperature 36 K, an identical mass and diameter of the clouds).

c) Star Formation in the Nuclear Molecular Disk

A large amount of molecular gas is packed in the nuclear disk. The high density of H_2 molecule suggests that active star formation (or starburst) occurs in the nucleus. The existence of a bright H II region (or an H II region complex) at the nucleus (Bonnarel, Boulesteix, and Marcelin 1986) supports active star formation. The size of the H II region is about 200 pc in diameter, which is roughly coincident with that of the nuclear disk. Turner and Ho (1983) observed radio continuum emission from the nuclear region at 6 cm and 2 cm and separated thermal from nonthermal components. Ten percent and 16% of the radio emission are of thermal origin at 6 cm and 2 cm, respectively. They estimated the number flux of UV photons to be $1.2 \times 10^{52} \text{ s}^{-1}$ which corresponds to 7×10^3 B3-O4 stars. This also supports active star formation in the nuclear region.

In the nuclear disk with a high H_2 density, cloud-cloud collisions probably occur frequently leading to massive star formations (Scoville, Sanders, and Clemens 1986). Also, a self-shielding effect possibly contributes to star-forming activity in the nuclear disk. UV photons from massive stars will dissociate hydrogen molecules and ionize hydrogen atoms. But by the effect of self-shielding, a large amount of molecules remains not dissociated at the nuclear region (see Elmegreen and Elmegreen 1987). Furthermore, a deep potential well observed as a large velocity gradient (see Fig. 2) in the nucleus may contribute to active star formation. A molecular cloud cannot escape from the nuclear disk region unless it is given a large kinetic energy. So a large amount of molecular clouds as fuel of star formation would remain and stay in the nuclear disk region until an explosive event like a starburst occurs.

d) Molecular Gas Bar and Formation of the Nuclear Molecular Disk

A plausible mechanism of formation of the nuclear molecular disk is gas infall caused by energy dissipation in shock waves formed in an oval stellar or gaseous gravitational potential as discussed by many authors. Sørensen, Matsuda, and

Fujimoto (1976) studied time evolution of the gas in a fixed potential of a bar and a disk and found that the shock waves are formed in the leading side of a bar which corresponds to the dark lanes in barred galaxies. Roberts, Huntley, and van Albada (1979) studied the steady state gas dynamics in a potential field with a moderate barlike perturbation and found a similar morphology of the shock waves as found by Sørensen, Matsuda, and Fujimoto (1976) and that ovally rotating supersonic gas is compressed at the shocks. At the shocks, gas dissipates energy and then infalls toward the galactic center. Combes and Gerin (1985) obtained similar results examining time-evolutionary response of dissipative gas cloud particles to the fixed stellar potential field. They suggested that one cloud collides with another when crossing the crowded region and dissipates energy to lose angular momentum.

The barlike structure seen in Figure 1*b* just fits to the theoretical morphology of the shock waves or the crowded structure of molecular clouds. When a radial motion of gas exists along a bar, the bar skews the isovelocity contours to lie more parallel to the major axis of the bar. The map of the isovelocity contours in Figure 1*c* indicates such an infall motion (or inward streaming motion along the bar). The nuclear molecular disk is probably formed up by gas accretion from the outer region. The strong central peaks in Figures 3*d*–3*h* might be caused by the accumulation of CO gas at the interfaces of the bar and the nuclear disk through the infall along the bar. If we assume that the observed “infall velocity” (see § III) is equal to the net velocity of infall motion, an upper limit of gas accretion

rate onto the nuclear disk is estimated to be about $10 M_{\odot} \text{ yr}^{-1}$. The structures of CO emission in IC 342 and Maffei 2 (Lo *et al.* 1984; Ishiguro *et al.* 1989) are also indicative of such a bar structure.

We observed that the gas within a radius of ~ 150 pc is circularly rotating. This is probably due to axisymmetry of the gravitational field in the nuclear disk; Shlosman, Frank, and Begelman (1989) claimed that asymmetry of the gravitational field no longer affect the motion of gas in such a central region. They suggested that the gas inflow in the barred potential slows down at the radius of about $0.1R_b$, where R_b is the radius of a stellar or gaseous bar, and a gaseous disk with a radial scale of $0.1R_b$ is formed. In case of NGC 6946, since the nuclear disk has a size of ~ 300 pc in diameter and the size of the oval potential is estimated to be larger than 1.7 kpc which is the apparent size of the molecular bar structure limited by the primary beam, the radius of the disk is smaller than $0.24R_b$.

Shlosman, Frank, and Begelman (1989) also suggest that, under certain conditions, the gaseous disk becomes dynamically unstable by an effect of self-gravity to form a smaller gaseous bar, and the smaller bar induces an infall motion of the gas and fuel an active galactic nucleus. In our results of NGC 6946, it is not clear whether the nuclear gas disk has a gaseous bar structure in it because of our limited angular resolution.

We are grateful to N. Nakai for fruitful discussions. We would like to thank the staff of NRO for development and maintenance of the NMA.

REFERENCES

- Ball, R., Sargent, A. I., Scoville, N. Z., Lo, K. Y., and Scott, S. L. 1985, *Ap. J. (Letters)*, **298**, L21.
 Bally, J., Stark, A. A., Wilson, R. W., and Henkel, C. 1988, *Ap. J.*, **324**, 223.
 Bonnarel, F., Boulesteix, J., and Marcellin, M. 1986, *Astr. Ap. Suppl.*, **66**, 149.
 Canzian, B., Mundy, L. G., and Scoville, N. Z. 1988, *Ap. J.*, **333**, 157.
 Chikada, Y., *et al.* 1987, *Proc. IEEE*, vol. 75, no. 9, p. 1203.
 Combes, F., and Gerin, M. 1985, *Astr. Ap.*, **150**, 327.
 de Vaucouleurs, G., de Vaucouleurs, A., and Corwin, H. G. 1976, *Second Reference Catalogue of Bright Galaxies* (Austin: University of Texas Press).
 Elmegreen, B. G., and Elmegreen, D. M. 1987, *Ap. J.*, **320**, 182.
 Gear, W. K., *et al.* 1984, *Ap. J.*, **280**, 102.
 Ishiguro, M., *et al.* 1984, in *Proc. Int. Symp. Millimeter and Submillimeter Wave Radio Astronomy*, ed. J. Gomes-Gonzales (Granada: URSI), p. 75.
 Ishiguro, M., *et al.* 1989, *Ap. J.*, **344**, 763.
 Ishiguro, M., *et al.* 1990, in preparation.
 Kawabe, R., *et al.* 1990, in preparation.
 Klein, U., Beck, R., Buczylowski, U. R., and Wielebinski, R. 1982, *Astr. Ap.*, **108**, 176.
 Knapp, G. R., Phillips, T. G., Huggins, P. J., Leighton, R. B., and Wannier, P. G. 1980, *Ap. J.*, **240**, 60.
 Lo, K. Y., *et al.* 1984, *Ap. J. (Letters)*, **282**, L59.
 Lo, K. Y., Cheung, K. W., Masson, C. R., Phillips, T. G., Scott, S. L., and Woody, D. P. 1987, *Ap. J.*, **312**, 574.
 Lo, K. Y., Phillips, T. G., Knapp, G. R., and Wootten, H. A. 1980, *Bull. AAS*, **12**, 859.
 Rickard, L. J., and Harvey, P. M. 1984, *A.J.*, **89**, 1520.
 Roberts, W. W., Huntley, J. M., and van Albada, G. D. 1979, *Ap. J.*, **233**, 67.
 Rogstad, D. H., and Shostak, G. S. 1972, *Ap. J.*, **176**, 315.
 Sandage, A., and Tammann, G. A. 1981, *A Revised Shapley-Ames Catalog of Bright Galaxies* (Washington D.C.: Carnegie Institution of Washington).
 Sanders, D. B., Scoville, N. Z., and Solomon, P. M. 1985, *Ap. J.*, **289**, 373.
 Scoville, N., Soifer, B. T., Neugebauer, G., Young, J. S., Matthews, K., and Yerka, J. 1985, *Ap. J.*, **289**, 129.
 Scoville, N. Z., Sanders, D. B., and Clemens, D. P. 1986, *Ap. J. (Letters)*, **310**, L77.
 Shlosman, I., Frank, J., and Begelman, M. C. 1989, *Nature*, **338**, 45.
 Sofue, Y., Doi, M., Ishizuki, S., Nakai, N., and Handa, T. 1988, *Pub. Astr. Soc. Japan*, **40**, 511.
 Sørensen, S.-A., Matsuda, T., and Fujimoto, M. 1976, *Ap. Space Sci.*, **43**, 491.
 Tully, R. B. 1988, *Nearby Galaxies Catalog* (Cambridge: Cambridge University Press).
 Turner, J. L., and Ho, P. T. P. 1983, *Ap. J. (Letters)*, **268**, L79.
 Ulich, B. L. 1981, *A.J.*, **86**, 1619.
 Weliachew, L., Casoli, F., and Combes, F. 1988, *Astr. Ap.*, **199**, 29.
 Young, J. S., and Scoville, N. 1982, *Ap. J.*, **258**, 467.

M. DOI and S. ISHIZUKI: Department of Astronomy, University of Tokyo, Bunkyo, Tokyo, 113, Japan

Y. CHIKADA, M. ISHIGURO, T. KASUGA, R. KAWABE, K.-I. MORITA, and S. K. OKUMURA: Nobeyama Radio Observatory, National Astronomical Observatory, Minamimaki, Minamisaku, Nagano, 384-13, Japan